Figure S1. Monocyte subset gating strategy by flow cytometry. Left panel, whole population of monocytes from human blood (isolated by elutriation); right panel, subset determination by staining with antibodies anti-CD14 and CD16. P1, whole population; P2, classical $CD14^{++}/CD16^{-}$ monocytes; P3, intermediate $CD14^{++}/CD16^{+}$ monocytes; P4, non-classical $CD14^{+}/CD16^{++}$ monocytes.

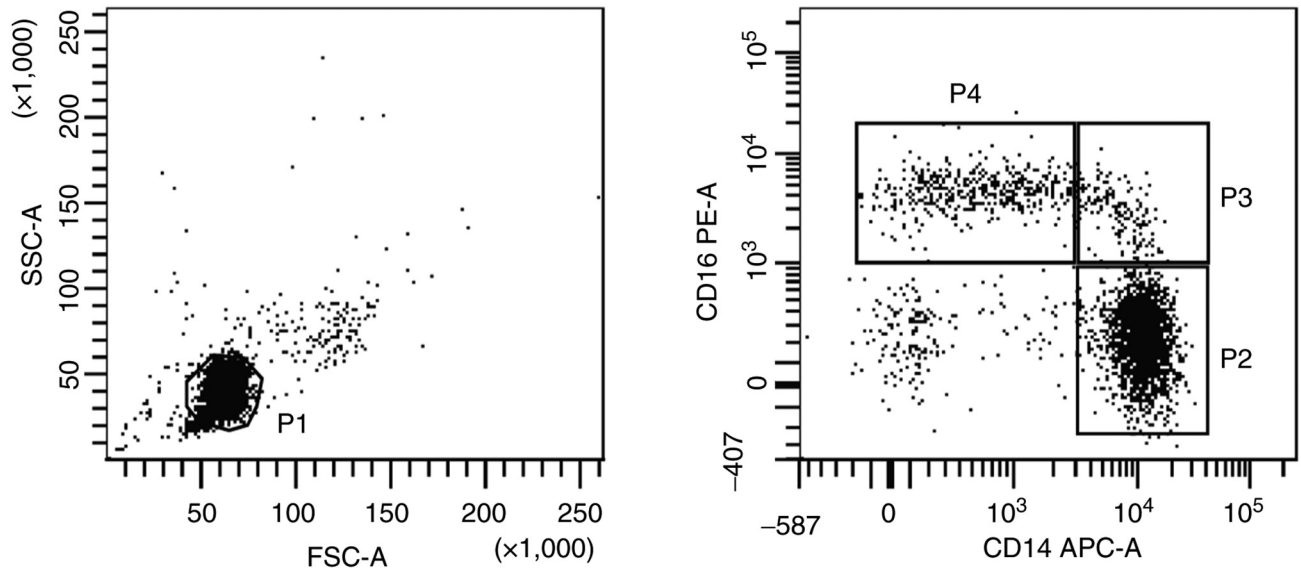

Figure S2. Representative nanoparticle tracking analysis measurement of $TEVs_{HCT116}$. (A and B) Sample video screenshots from the NTA measurement obtained with NanoSight LM10HS equipped with the LM14 488-nm laser module (Malvern Instruments, Ltd.).

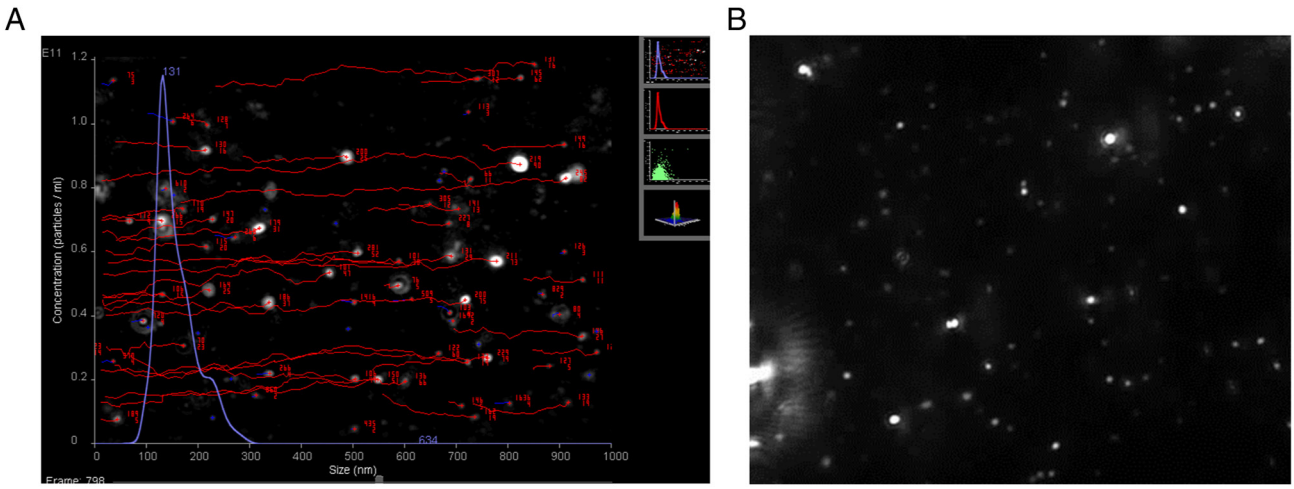

Figure S3. Efficiency of $TEVs_{HCT116}$ labeling with SYTO RNASelect dye by NTA and flow cytometry. (A) Representative NTA size profile of $TEVs_{HCT116}$ without dye. (B) Representative NTA size profile of SYTO RNA-labeled $TEVs_{HCT116}$. (C) Representative histogram of $TEVs_{HCT116}$ in FL1 channel without labeling. (D) Representative histogram of SYTO RNA-labeled TEVsHCT116 in FL1 channel. NTA, nanoparticle tracking analysis; TEVs, tumor-derived extracellular vesicles.

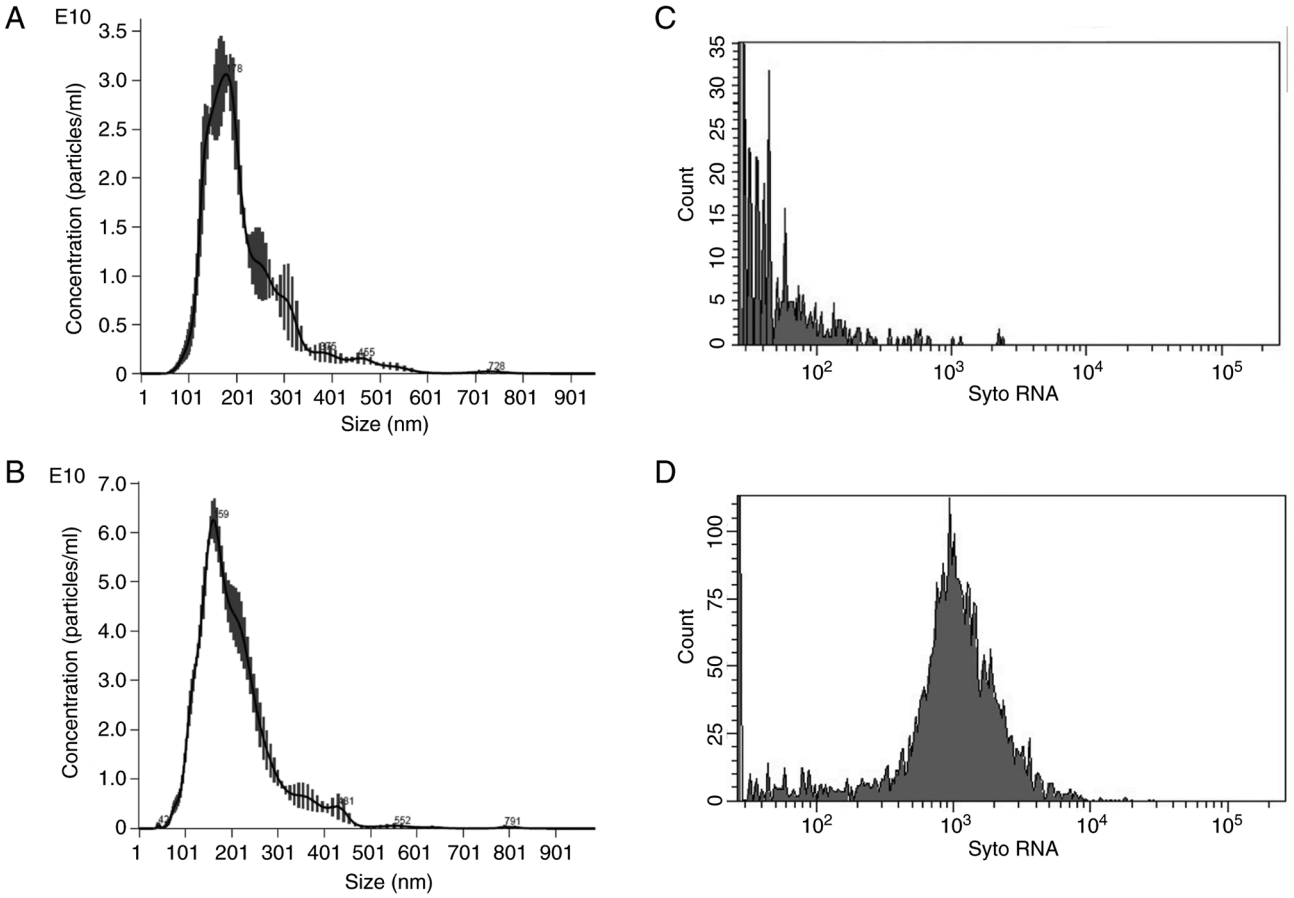

Figure S4. Representative CD44 expression on monocytes after 0, 2 and 18 h incubation at 37˚C.

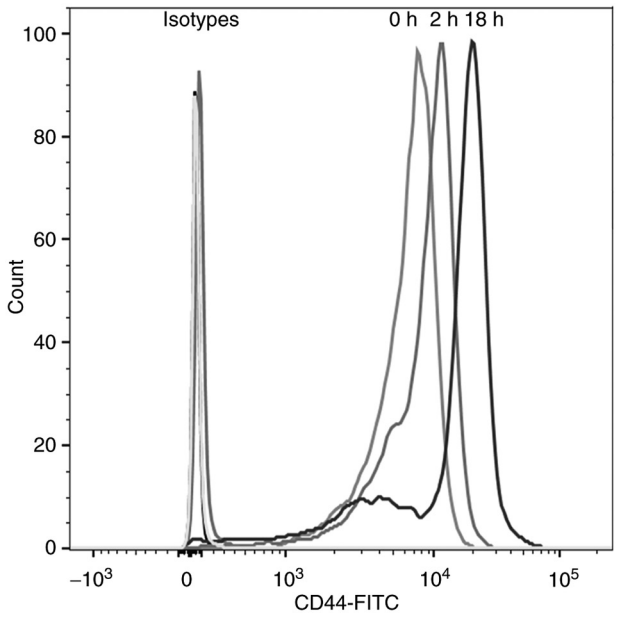

Figure S5. Kinetics of $TEVs_{HCT116}$ and $TEVs_{SW1116}$ attachment to monocytes. Data are presented as the mean ± SEM of three experiments. TEVs, tumor-derived extracellular vesicles; MFI, mean fluorescence intensity.